Revue-IRS

Revue Internationale de la Recherche Scientifique (Revue-IRS)

ISSN: 2958-8413

Vol. 4, No. 6, Novembre 2026

This is an open access article under the CC BY-NC-ND license.

Modeling and Forecasting the Trajectories of Cyclonic and Anticyclonic Vortices Using LSTM

ABDALLAH Salim S.O.*[1, 2], LALAOHARISOA Sahoby[1], RANDRIANARISON Hervais Dieu Donné[1], SALIM Ahmed Ali[2], RATIARISON Adolphe A[1].

[1]Atmosphere, Climate, and Ocean Dynamics laboratory, Doctoral School of Physics and Applications, University of Antananarivo, Antananarivo, Madagascar.

[2]Environmental and Climate Physics Laboratory, Faculty of Science and Technology, University of the Comoros, Moroni, Comoros.

Corresponding author: ABDALLAH Salim S.O,

Abstract: This study presents an approach based on Long Short-Term Memory (LSTM) recurrent neural networks to model and predict the trajectories of cyclonic and anticyclonic vortices in the northern Mozambique Channel. Multivariate oceanographic data (longitude, latitude, sea surface temperature (SST), surface salinity (SSS), and surface anomalies) were preprocessed and analyzed using Granger causality to validate the interdependencies between variables. A two-layer stacked LSTM model was trained on 70% of the data, validated on 15%, and tested on the remaining 15%. The results show remarkable performance: $R^2 > 0{,}850$ for cyclones and $R^2 > 0{,}900$ for anticyclones, with MAPE errors slightly above 1% for anticyclones in terms of latitude, and below 1% for the rest. The five-day forecast for the year 2020 confirms that this method effectively predicts short-term changes in ocean dynamics.

Keywords: oceanic eddy, LSTM, trajectory forecasting, Granger causality, anomaly

Digital Object Identifier (DOI): https://doi.org/10.5281/zenodo.24564189

1 Introduction

Ocean eddies play a fundamental role in the redistribution of heat, nutrients, and water masses in the Indian Ocean. In the northern part of the Mozambique Channel, these structures take two main forms: cyclonic eddies, characterized by counterclockwise rotation associated with upwelling, and anticyclonic eddies, characterized by clockwise rotation associated with downwelling [1].

Predicting the trajectories of these structures remains difficult due to the complexity of oceanic movements and the interactions between physical variables (SSS, SSH, ocean currents, SST, etc.) [2], [3].

Traditional numerical modeling methods, while effective, require high computational power and involve large-scale interactions. Given these limitations, Long Short-Term Memory (LSTM) recurrent neural networks offer a suitable alternative for analyzing time series with long-term dependencies.

2 Material and methods

2.1 Study area and data

2.1.1 Geographic area

Our study area covers the northern part of the Mozambique Channel, corresponding to the geographical band between latitudes 8°S and 16°S and longitudes 40°E and 50°E. This region is known for its high concentration of eddies, fed by the western boundary currents of the Indian Ocean, particularly the Mozambique Current. The eddies that form there have lifespans ranging from a few weeks to several months and generally migrate toward the southwest [4].

2.1.2 Oceanographic variables used

The input variables for the model are as follows:

- Longitude and Latitude: geographic coordinates of the vortices' centers;
- Sea Surface Temperature (SST): a thermal indicator of the vortices' structure;
- Sea Surface Salinity (SSS): reflects the exchange between freshwater and saltwater;
- Sea surface height: a marker of the dynamic structure of the eddies;
- Surface ocean current speed and wave height: kinematic parameters associated with the intensity of the eddies;
- Surface area of vortices (cyclonic or anticyclonic).

2.2 Methodology

This study is based on the preprocessing of oceanographic data, Granger causality analysis, and the development of an LSTM neural network for forecasting eddy trajectories. The model was trained, validated, and tested according to a rigorous protocol. The chosen architecture was selected based on the characteristics of the dataset and its predictive performance [5].

2.2.1 Data preprocessing

Before training the LSTM model, the data underwent a preprocessing step to improve its quality, standardize its representation, and adapt it to the input format required by the neural network.

- ❖ Imputation of missing values via temporal interpolation;
- ❖ Min-Max normalization or standardization (z-score) to standardize the scales;
- ❖ Transformation into sliding time series of length n_timesteps;
- ❖ Conversion to cell array format for MatLab: each cell contains a sequence [n_features × seq_len].

2.2.2 Granger causality analysis

The causality test was applied to validate the relationships between the various oceanographic variables and justify their inclusion in the model [5].

A p-value of zero indicates two-way causality between all pairs of variables for both cyclonic and anticyclonic vortices.

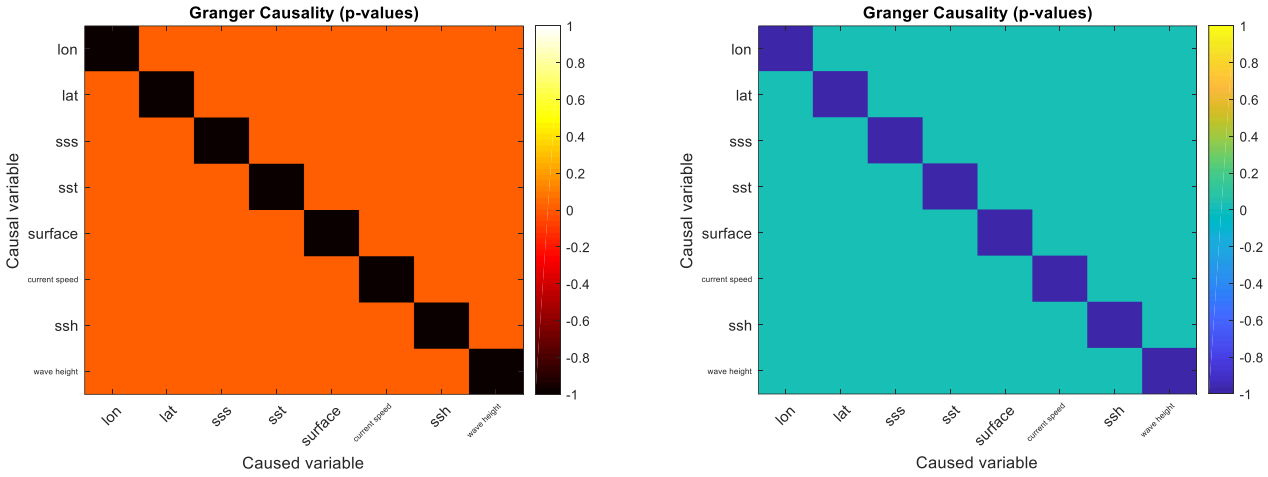

Cyclonic vortices Anticyclonic vortices

Figure 1. Granger Causality Matrix for Vortices

The Granger causality matrix shows zero p-values for all off-diagonal pairs. This indicates bidirectional causal relationships between longitude, latitude, SSS, SST, SSH, and wave. Each variable provides useful information for predicting the system, which justifies the use of a multivariate model.

In cyclonic eddies, we observe surface cooling, upwelling of deep water, and negative SSH anomalies that sustain the eddies' dynamics. In contrast, anticyclonic eddies are characterized by sea surface warming, positive SSH anomalies, and surface water convergence, while maintaining a close coupling between the variables.

2.2.3 LSTM model architecture

The architecture of the model used consists of one or more LSTM layers followed by fully connected (dense) layers, which enable the learned temporal representations to be transformed into predictions of the geographical coordinates of vortices. The input sequence consists of a time window of past observations, and the output corresponds to the forecast of future positions. This methodological choice effectively incorporates temporal memory and the nonlinearity of the variables, thereby providing a robust approach for short- and medium-term ocean simulation and forecasting [6], [7], [8].

Five LSTM architectures were evaluated based on the complexity of the time series (as shown in the following flowchart).

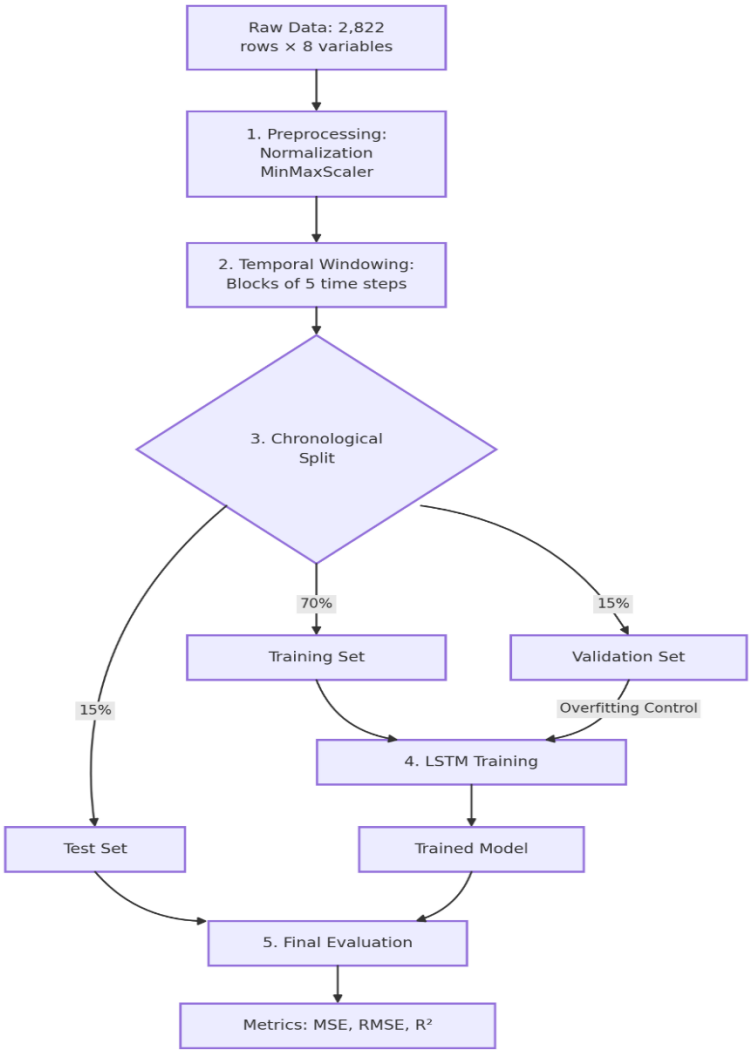

Figure 2. Processing flowchart for the LSTM model architecture

2.2.4 LSTM mathematical model

Each LSTM cell consists of three main gates: the forget gate, the input gate, and the output gate, which regulate, respectively, the retention of past information, the integration of new information, and the generation of the output. These mechanisms enable the retention of relevant information, the integration of new knowledge, and the generation of an appropriate output, thereby ensuring the modeling of long-term temporal dependencies.

The update of the cell's state is formulated to retain relevant information over long periods while discarding obsolete data, thereby enabling the capture of the complex, nonlinear dynamics of the ocean system.

Each LSTM cell is governed by four fundamental equations:

- ✓ **Forget Gate**: This gate evaluates information from the previous cell state and determines which information should be retained or discarded, based on its relevance to the learning task [8], [9], [10].

$$f_t = \sigma(W_f \cdot [h_{t-1}, x_t] + b_f) \quad (1)$$

Where W_f is the learned weight matrix for the forget gate;

b_f is the learned bias vector for this gate;

x_t is the input (a vector of the six current observations);

h_{t-1} is the previous hidden state: a representation of the information already processed.

- ✓ **Input Gate:** It controls the incorporation of new information into the cell state by selecting relevant data from the current input and the previous hidden state [8], [9], [10].

$$i_t = \sigma(W_i \cdot [h_{t-1}, x_t] + b_i)$$
$$\tilde{C}_t = \tanh(W_C \cdot [h_{t-1}, x_t] + b_C) \quad (2)$$

W_i: weight matrix of the input gate;
b_i: bias vector of the input gate;
b_c: associated bias vector;
W_c: weight matrix for constructing the candidate content.

- ✓ **Output Gate:** This gate selects the cell state information to be transmitted as a hidden state, which is used to generate the network's output and feed the next time step [8], [9], [10].

$$o_t = \sigma(W_o \cdot [h_{t-1}, x_t] + b_o) \quad (3)$$

Where σ is the sigmoid function,
o_t: coefficients that control the information revealed in the hidden state;
W_o: output gate weight matrix;
b_o: output gate bias vector;

- ✓ **Updating the memory status:** $C_t = f_t * C_{t-1} + i_t * C_t \quad (4)$

C_t: updated internal memory;
C_{t-1}: internal memory before the update;
$\tilde{C}_t$: new content proposed for the memory

II-2-5. Training and Forecasting

The model was trained using the following hyperparameters, determined by cross-validation:

- Optimizer: ADAM (Adaptive Moment Estimation);
- Loss function: MSE (Mean Squared Error);
- Number of epochs: 100;
- Mini-batch size: 64;
- Gradient threshold: 1;
- Initial learning rate: 0.005.

A recursive forecasting strategy was adopted: the last known sequence is used to predict the next time step, which is then fed back as input for subsequent predictions, thereby enabling projections several days in advance.

2.2.5 Selection and optimization of the neural network architecture

The two-layer LSTM architecture was chosen because it offers a good balance between learning capacity and generalization. It is well-suited to the complexity of oceanographic variables and the limited size of the dataset.
The first LSTM layer (64 neurons) extracts temporal dependencies. The second layer (32 neurons) summarizes the information relevant to the prediction. A dense layer of 16 neurons with the ReLU activation function enhances the data representation before the output. The final layer consists of two neurons, corresponding to latitude and longitude [10], [11].

3 Results

The modelling results are presented following the successive stages of data preprocessing, analysis, and processing.

3.1 Model performance

The stacked LSTM architecture delivers excellent results for predicting vortex structures, although there are some nuances depending on their nature:

- Cyclonic vortices: The model demonstrates exceptional performance and maximum accuracy for these.
- Anticyclonic vortices: Performance is high, although slightly lower than that obtained for cyclones.

Table 1. Performance metrics of the LSTM model for vortices

Vortices	Indicator	Latitude	Longitude
Cyclones	R^2	0,990	0,990
	MAPE	0,374 %	0,217 %
Anticyclones	R^2	0,971	0,983
	MAPE	0,939 %	0,266 %

3.2 Training: 70%

Figure 3 illustrates the training phase of the LSTM model. It accurately reproduces the movement of mesoscale structures in the northern part of the Mozambique Channel. The predicted trajectories (red) closely follow the actual trajectories (blue).

High-pressure systems show a distinct drift. Their latitude shifts from 12°S to 16°S, and their longitude from approximately 48°E to 42°E. They are therefore moving toward the southwest. Cyclones are more irregular. They move back and forth in latitude between 13°S and 16°S. The vertical jumps mark the transition from one vortex to another.

However, this strong performance during the training phase is only a necessary but not sufficient condition for the model's quality: it must be confirmed on unseen data; otherwise, it could simply be a result of overfitting. This is precisely the purpose of the subsequent validation and testing phases.

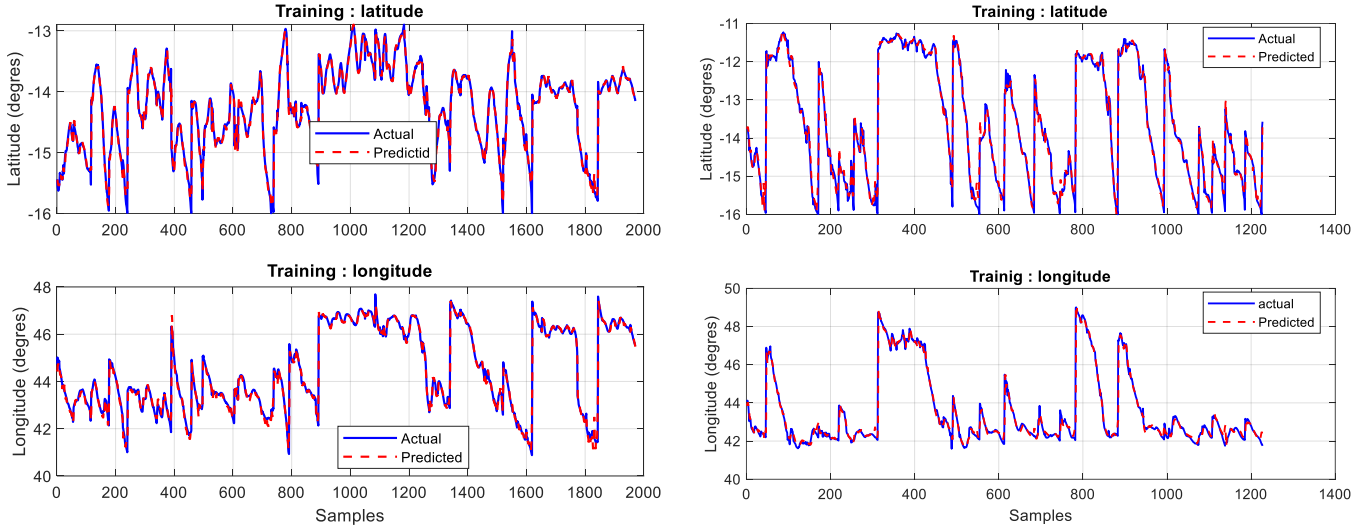

cyclones Anticyclones

Figure 3. Schematic representation of the LSTM model training proces

3.3 Validation: 15%

During the validation phase shown in Figure 4 (15% of data not seen), the model maintains excellent predictive performance and confirms its good generalization without overfitting, despite a slight, expected decline in accuracy.

For cyclones, the agreement is very good. Small discrepancies appear during rapid troughs (for example, around sample 135 in longitude). The model predicts a shallower trough there than the actual trough. For high-pressure systems, the agreement is good, with a few isolated outliers. Around sample 65, the predicted longitude rises to 45,5°E instead of approximately 43,5°E. At the end of the series, the predicted latitude deviates by about 1° from the actual value. These outliers occur at the change of vortex.

The absence of any significant deterioration in performance metrics between the training and validation phases is a significant finding: it demonstrates that the stacked LSTM model has indeed learned a generalizable representation of vortex dynamics, rather than simply memorizing the training trajectories. This result reinforces the validity of the architectural choice and the data preprocessing strategy that were implemented.

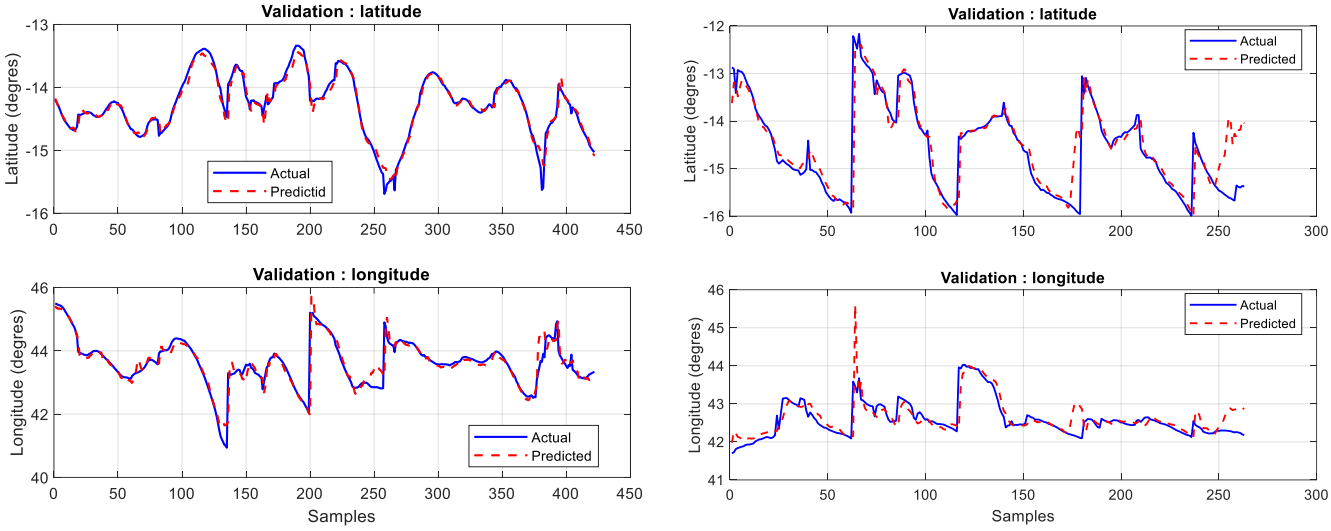

Cyclones Anticyclones

Figure 4. Illustration of the validation procedure of the LSTM model

3.4 Test: 15%

Figure 5 shows the testing phase of our model. For cyclones, the model closely matches the data up to approximately sample 375. The last track is very different from the others. It lies farther north, around 9,5°S - 10°S, and farther east, around 49°E - 50°E. In the training data, cyclones do not extend beyond approximately 13°S and 47,5°E. The deviation reaches nearly 2° in both latitude and longitude, or more than 200 km. This single track most likely explains the lower R^2 at lower latitudes for cyclones (0,862). For anticyclones, the test performs very well. We see only an isolated peak in longitude around sample 195, at the change in vortex.

Despite these slight local discrepancies, the model's overall consistency over time and space remains excellent. This is confirmed by the high accuracy of the longitude measurement, with a mean absolute percentage error (MAPE) of only 0,266%.

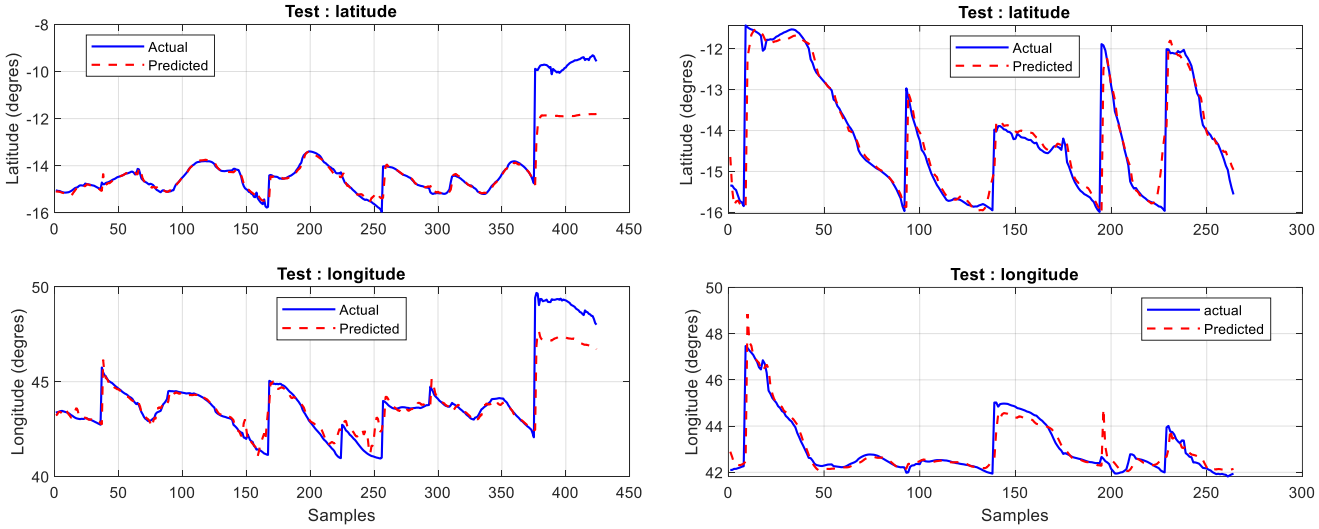

Cyclones Anticyclones

Figure 5. Schematic overview of the LSTM model testing phase

3.5 Trajectory prediction for 2020

The forecast phase of our LSTM model for vortices is shown in Figure 6, with the actual track (blue) and the LSTM forecast shown as red dots. For the 5-day forecast in 2020, the model demonstrates its operational capability while revealing distinct behaviors depending on the nature of the structures.

The cyclonic vortex is located near 9,5°S and 48°E. Its observed track is irregular, with loops near 49,3°E. The forecast indicates it will continue westward. It is moving about 0,3° every 5 days, or approximately 7 km per day. This direction is consistent with its most recent observed movement.

The anticyclonic gyre is moving from the northeast (44°E: 12°S) toward the southwest (42°E: 15,5°S). The forecast remains around 15°S - 15,2°S and 42°E - 42.2°E. It does not continue moving southward. It remains close to its last position, with a slight return toward the north. This behavior may be due to the proximity of the southern edge of the study area (16°S).

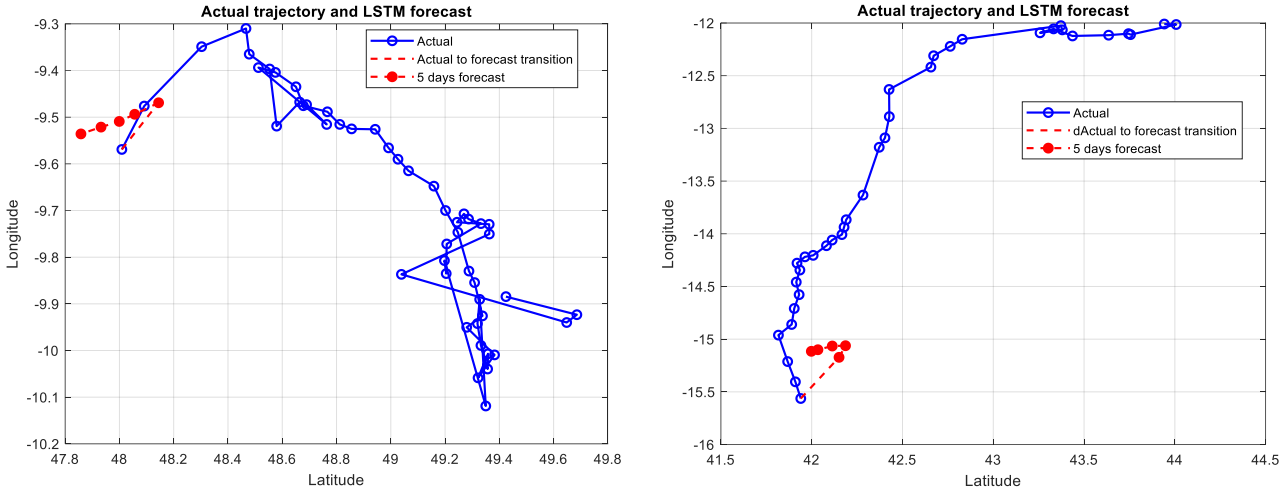

cyclones Anticyclones

Figure 6. Visualization of the LSTM model's forecast

4 Discussion

The results show that the LSTM model performs well in predicting the trajectories of oceanic vortices. The R^2 values range from 0,862 to 0,955. They confirm the model's ability to accurately reproduce the movements of cyclones and anticyclones.

The five-day forecast shows average errors of 44,3 km for cyclones and 37,3 km for anticyclones. Anticyclones are therefore predicted with greater accuracy. This difference may be due to the more erratic variations in cyclone tracks.

Despite this performance, the model has certain limitations. It has difficulty reproducing sudden changes in direction and unusual trajectories. These discrepancies show that the dynamics of vortices remain difficult to predict.

Improving the model requires the incorporation of new physical variables and the development of hybrid architectures. These approaches could improve forecast accuracy and better represent the spatiotemporal dynamics of vortices.

5 Conclusion

This study shows that LSTM neural networks are an effective approach for modeling and forecasting the trajectories of ocean eddies in the northern Mozambique Channel. The multivariate approach allows for the consideration of interactions between different physical variables.

Granger causality tests also reveal statistically significant relationships between the variables under consideration ($p = 0$), for both cyclones and anticyclones.

The model's performance is satisfactory. For cyclones, the R^2 coefficients are 0.862 for latitude and 0.946 for longitude. The corresponding MAPEs are 0.374% and 0.757%. For anticyclones, the R^2 values are 0.945 and 0.955, respectively, with MAPEs of 1.085% and 0.354%.

The five-day forecasts generated in 2020 confirm the model's ability to reproduce realistic and consistent trajectories. These results contribute to the application of deep learning methods to the study of ocean eddy dynamics.

Future research will focus on the use of higher-resolution data, improving long-range forecasts, and studying the interactions between cyclones and anticyclones.

REFERENCES

[1] Y. S. José, O. Aumont, E. Machu, P. Penven, C. L. Moloney, et O. Maury, « Influence of mesoscale eddies on biological production in the Mozambique Channel: Several contrasted examples from a coupled ocean-biogeochemistry model », *Deep Sea Res. Part II Top. Stud. Oceanogr.*, vol. 100, p. 79-93, févr. 2014, doi: 10.1016/j.dsr2.2013.10.018.

[2] « (PDF) Prévision à moyen terme de la trajectoire des tourbillons océaniques ». Consulté le: 5 novembre 2026. [En ligne]. Disponible sur: https://www.researchgate.net/publication/377281200_Medium-range_forecasting_of_oceanic_eddy_trajectory

[3] « Time Series Forecasting Using Deep Learning - MATLAB & Simulink ». Consulté le: 5 novembre 2026. [En ligne]. Disponible sur: https://www.mathworks.com/help/deeplearning/ug/time-series-forecasting-using-deep-learning.html

[4] M. W. Schouten, W. P. M. de Ruijter, P. J. van Leeuwen, et H. Ridderinkhof, « Eddies and variability in the Mozambique Channel », *Deep Sea Res. Part II Top. Stud. Oceanogr.*, vol. 50, nº 12, p. 1987-2003, juill. 2003, doi: 10.1016/S0967-0645(03)00042-0.

[5] M. AIT OUDRA et D. Ibrahim, « Cointégration et causalité entre gouvernance et croissance économique: Cas du Maroc », *Rev. Contrô Comptab. L'Audit*, vol. 3, nº 3, 2019, Consulté le: 23 octobre 2026. [En ligne]. Disponible sur: https://www.revuecca.com/index.php/home/article/view/391

[6] MEZAACHE Ahmed, « Classification Des Données Basée Sur Les Réseaux De Neurones Récurrents (RNN) ». Faculté des Sciences et de la Technologie - Département de Génie Electrotechnique et Automatique, Université 8 Mai 1945 – Guelma - République Algérienne Démocratique et Populaire, 2024 2023.

[7] T. Stérin, « Réseaux de neurones récurrents et mémoire : application à la musique », sept. 2016, [En ligne]. Disponible sur: http://www.telecom-bretagne.eu/

[8] R. Zard, « Analyse des données actimétriques et prédiction par LSTM des phases de sommeil chez une population âgée institutionnalisée ». ÉCOLE DOCTORALE 548 Mer et Sciences, Université de Toulon, décembre 2024.

[9] Kalidou Moussa SOW, « MODELISATION STATISTIQUE ET PREDICTION PAR APPRENTISSAGE AUTOMATIQUE : LA DEGRADATION PAR APPLICATION A LA CORROSION D'UN PIPELINE ». UNIVERSITE DU QUEBEC, décembre 2024.

[10] « LSTM: Long Short-Term Memory - une mémoire longue durée pour les séquences ». Consulté le: 24 octobre 2026. [En ligne]. Disponible sur: https://www.chiny.me/lstm-long-short-term-memory-une-memoire-longue-duree-pour-les-sequences-27-18.php

[11] « Modèles LSTM : guide complet des réseaux à mémoire à long et court terme ». Consulté le: 24 octobre 2026. [En ligne]. Disponible sur: https://www.datacamp.com/tutorial/lstm-models